JOURNAL OF MATERIALS SCIENCE **40** (2005) 4287–4291

Synthesis and structure of multi-layered WS_2(CoS), MoS_2(Mo) nanocapsules and single-layered WS_2(W) nanoparticles

P. Z. SI, M. ZHANG, Z. D. ZHANG, X. G. ZHAO, X. L. MA, D. Y. GENG
Shenyang National Laboratory for Materials Science, Institute of Metal Research, and International Centre for Materials Physics, Chinese Academy of Sciences, Shenyang 110016, China
E-mail: pzsi@imr.ac.cn

Multi-layered MoS_2 (or WS_2) nanocages stuffed with Mo (or CoS/CoO) nanocrystals have been synthesized by using the reaction between metal nanoparticles and sulfur powders. This simple synthesis method, different from the conventional methods for synthesizing pure inorganic fullerenes, is also potentially important for large-scale synthesis of nanoparticles of other metal dichalcogenide. Besides the multi-layered WS_2 nanocapsules, we have successfully fabricated nanocapsules with a single-layered WS_2 sheet encapsulating W by using the arc-discharge method. We discuss possible mechanisms for the formation of the unique core-shell structured nanocapsules.

1. Introduction

The encapsulation of nanocrystallite materials is important, not only in scientific research because of the novel properties induced by size-, surface- and interface-effects, but also in many technologies, ranging from cluster protections, catalysts to biomedical applications [1]. Recently, one focuses for encapsulation on materials with a layered structure because of their bendable layers in nanoscale. To date, a great number of nanoscale materials have been successfully encaged in curled-up graphite and *h*-BN layers [1–3]. However, it is still difficult for synthesis reasons to have a universal encapsulation of foreign nanoparticles with metal dichalcogenides (MX_2, M = W, Mo, Nb, Ta; X = S, Se, Te), even though they show analogous layered structures to graphite and *h*-BN. On the other hand, the most effective method for synthesizing pure fullerene-like WS_2 and MoS_2 materials are based on solid-gas reactions, in which a large amount of H_2S and/or H_2 are used as reducing agents in conjunction with metal compounds as precursors [4, 5]. For example, by annealing oxide precursors in flowing $H_2S + H_2$, one can produce about one gram of hollow WS_2 nanoparticles with a relatively broad size distribution [5]. Although recent modifications to this method have to some extent scaled up the production, a large amount of H_2S and H_2 are still needed to provide elemental sulfur and reducing agents [6]. Other techniques, including electron-beam irradiation [7], sonoelectrochemical bath reaction [8], electron chemical deposition [9], and C_{60} catalyzed self-assembly process [10], have also been developed to grow a small amount of pure inorganic fullerenes. In a word, most of the research in this field is focused on the synthesis of multi-layered pure inorganic fullerenes, which are spherical or tubular in shape.

In this work, we report a novel method for the large-scale synthesis and the structural properties of nanocapsules with WS_2 (or MoS_2) shell material encapsulating CoS/CoO (or Mo) cores, and show that the rapidity of this method, simplicity of the reactors, nonuse of H_2 and minimized usage of H_2S make the present method a powerful synthesis route. In the following, we annotate the shell core structure by setting the shell composition before the core composition in brackets "shell (core)". Besides the multi-layered WS_2(CoS/CoO) and MoS_2(Mo) nanocapsules, single-layered WS_2 (W) nanocapsules have been fabricated by using the arc-discharge method.

2. Experimental procedure

2.1. Synthesis of multi-layered WS_2(CoS/CoO) nanocapsules

Nanocapsules consisting of multi-layered WS_2 shells which encapsulate CoS/CoO nanoparticles (hereafter S1) were produced by reaction between cobalt (doped with elemental tungsten) nanoparticles and sulfur powders. In analogy with our previous work [2, 3], the W-doped cobalt nanoparticles were prepared via the arc-discharge method, in which a cobalt cylinder compacted with 99 wt% purity Co powders was used as anode while a 1.5 mm-diameter W needle was used as cathode, an arc-discharge with a typical current of 300 A was maintained for 2 h in an argon atmosphere. The W-doped cobalt nanoparticles generated by arc discharge were then mixed with excess commercial

sulfur powders in an ultrasonic alcohol bath. After the mixing process, the alcohol was evaporated in a boiling water bath. Finally, the dried mixture was heated up to about 600°C for 1 h, using a resistance heater placed in a water-cooled chamber (Φ28 cm × 40 cm) filled with an atmosphere of Ar (10000 Pa) + H_2S (4000 Pa).

2.2. Synthesis of multi-layered MoS_2(Mo) nanocapsules

In analogy to the preparation of sample S1, nanocapsules consisting of multi-layered MoS_2 shells which encapsulate Mo nanoparticles (hereafter S_2) were prepared by reaction between Mo nanoparticles and sulfur powders. The Mo nanoparticles precursor was also prepared via the arc discharge method, in which bulk Mo and a 4 mm-diameter W needle were used as anode and cathode, respectively. The Mo nanoparticles prepared this way were mixed with excess sulfur powders in an ultrasonic alcohol bath. Then the alcohol was evaporated in a boiling water bath. After that, the dried mixture was heated up to about 600°C for 1 h, using a resistance heater placed in a water-cooled chamber (Φ28 cm × 40 cm) filled with an atmosphere of Ar (10000 Pa) + H_2S (4000 Pa). In fact, the reaction processes to generate S1 and S2 were carried out using the same heater and at the same time.

2.3. Synthesis of single-layered WS_2(W) nanocapsules

The W nanoparticles coated with single-layered WS_2 sheet (hereafter S3) were synthesized via an arc-discharge method. An arc-discharge with a typical current of 300 ampere, maintained for 2 h, was struck between the bulk tungsten anode and tungsten needle cathode in an atmosphere of Ar (12000 Pa) + H_2S (3000 Pa). After the experiments, the waste gas in the chamber was pumped out and then the powder products on the chamber wall were collected in air and used in the further experiments.

2.4. Characterization

X-ray powder diffraction (XRD) experiments on S1, S2, W-doped cobalt nanoparticles, and Mo nanoparticles, respectively, were conducted to identify the phases in the products and lattice parameters. The shell-core structures of the nanocapsules S1, S2, and S3 were investigated by using high-resolution transmission electron microscopy (HRTEM) (Jeol type JEM2010).

3. Results and discussion

3.1. Multi-layered WS_2(CoS/CoO) nanocapsules

Fig. 1 shows the XRD spectra of the precursor metal nanoparticles and the final sulfuration products. Cobalt and cobalt oxide could be indexed in the XRD spectra of the precursor cobalt nanoparticles, as shown in Fig. 1c. The presence of the cobalt oxide in the precursor should

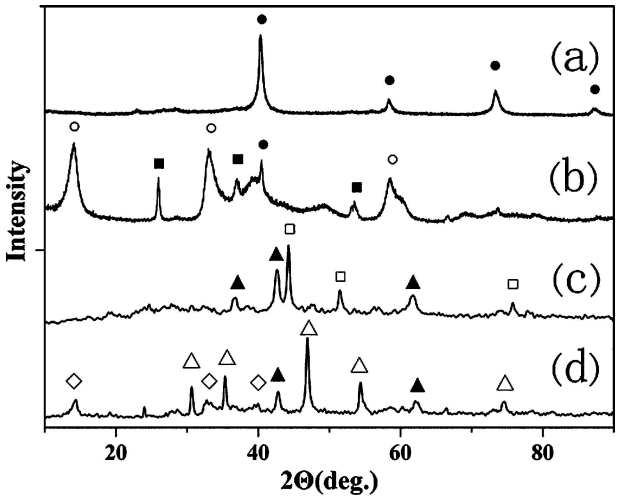

Figure 1 Normalized X-ray diffraction patterns of (a) the precursor Mo nanoparticles; (b) the reaction products between (a) and sulfur powders; (c) precursor W-doped cobalt nanoparticles; and (d) products of the reactions between (c) and sulfur. ● Mo; ○ MoS_2; ■ MoO_2; □ Co; ▲ CoO; △ CoS; ◇ WS_2.

be mainly ascribed to the evaporation of oxide in the commercial cobalt powders. Of course, when exposed to air, the atoms on the fresh surface of the metallic cobalt nanoparticles would also be partially oxidized by oxygen. Although no tungsten has been detected by XRD in the cobalt nanoparticles, nonetheless, both the XRD and TEM results of S1 verified the presence of elemental tungsten in the precursor. In fact, during the arc discharge process, the 1.5 mm-diameter tungsten needle had been obviously shortened after the experiment, indicating the tungsten evaporation and thus doping to the cobalt nanoparticles.

Sample S1 consists of three phases, i.e. WS_2, CoS and CoO, as shown in Fig. 1d. The HRTEM observations shown in Fig. 2, illustrate the structure and the phase distribution of the S1 nanoparticles. It is revealed that most of the S1 particles have core/shell structures, where the shell is the layered WS_2. Although different shapes of the WS_2 (CoS/CoO) nanocapsules are observed (Fig. 2.), their sizes are usually less than 95 nm, while the shells consist of 4–10 layers of WS_2 sheets. For nanoparticles with polyhedral shape, WS_2 sheets spread over the particle surfaces and thus apexes are formed (Fig. 2a). A smaller spherical nanocapsule (Fig. 2b) suggests that the spherical shape might be more stable for very small nanocapsules, owing to the annihilation of the WS_2 dangling bonds. We attribute the formation of the elongated tubular nanocapsules to the large original particle size or possibly the contact of different particles (Fig. 2c). It is noticed that mismatch and breakdown of WS_2 sheets are frequently observed at the apex areas and quite small nanocapsules. We attribute this phenomenon to the occurrence of internal pressure. The strain relief of the folding structure and the volume expansion during the sulfuration process may result in an internal pressure.

The growth mechanism of the WS_2 (CoS/CoO) nanocapsules is not fully understood yet. However, it is clear that most of the WS_2 phase is presented on the

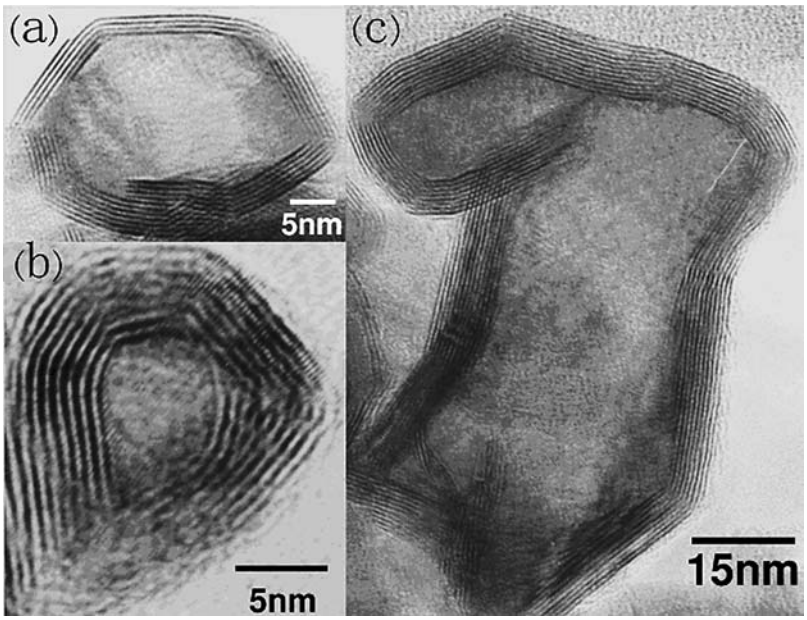

Figure 2 TEM images of multi-layered WS_2 encapsulating CoS/CoO nanocapsules with (a) polyhedral shape (30 nm in diameter); (b) spherical shape (17 nm in diameter); and (c) elongated shape (95 nm in length).

particle surface as shell, indicating a higher stability of the core/shell structure instead of others e.g. intercalated structures. We tend to believe that the products are formed in two steps. The first step is a surface reaction, during which the surface atoms of cobalt and tungsten react quickly with sulfur. The nanoparticles are partially coated by WS_2 monolayers at this stage. The second step involves atom diffusion, phase segregation and a template growth of WS_2 shells. At elevated temperatures, sulfur atoms diffuse through the previously formed sulphide and react with the metals inside the nanoparticles. Since tungsten is not necessarily to be presented merely on the particle surface, therefore the *in situ* formed WS_2 would combine their dangling bonds with the surface WS_2 to form a more stable structure. TEM observations also show an almost uniform shell and intimate contact of the shell and the core. These phenomena suggest that the CoS core serves as a template for WS_2 growth. The obviously observed mismatch and stacking of the WS_2 sheets over the particle surface indicates that the WS_2 shell most probably grows from different WS_2 nuclei.

3.2. Multi-layered MoS_2(Mo) nanocapsules

The XRD spectra verify that the Mo nanoparticles used to generate S_2 consists of well-crystallized Mo phase, as shown in Fig. 1a. No molybdenum oxides were detected in the precursor Mo nanoparticles. The S_2 products of the reactions between Mo nanoparticles and sulfur powders consist of MoS_2, Mo, and a small amount of MoO_2, as shown in Fig. 1b. Two reasons should be responsible for the presence of MoO_2 in the final product. On the one hand, fresh Mo surface would be oxidized spontaneously when exposed to air, even though its oxide was not detected by XRD in the precursor Mo nanoparticles, owing to its limited thickness and/or low percentage in weight. On the other hand, Mo nanoparticles would react with remains of oxygen in the chamber or physically absorbed on the particle surfaces at elevated temperatures, owing to the limited vacuum.

The conventional direct solid-state reactions, for example, $Mo + S \rightarrow MoS_2$ [11], are often complicated by the need for long reaction times at elevated temperatures, owing to a limited amount of intimate contact between solid reactants and too long diffusion lengths. Our present reactions, however, largely enhance the kinetic conditions, because of a much larger surface area and small size of the metal nanoparticles used as precursors.

Fig. 3a shows a typical spherical onion-like MoS_2(Mo) nanocapsule. The well-established concentric rings in the outer part of the nanocapsules are projections of the basal planes of MoS_2 parallel to the beam. Besides the ideal spherical nanocapsules, we also observed the elongated tubular shape nanocapsules, as shown in Fig. 3b. The formation of tubular nanocapsules should be attributed to the contact of the Mo nanoparticles during synthesis. The electron diffraction experiment also verifies that the shell is composed of MoS_2 (Fig. 3c). The TEM observations show a narrow size distribution (15–45 nm) of the products. Moreover, the MoS_2 nanocapsules, compared with the original Mo nanoparticles (9 nm in average size), show a relatively larger size, owing to the expansion of volume during sulfuration. Most shells of the nanocapsules are MoS_2, while the cores are Mo/MoO_2, because any fresh Mo/MoO_2 surface would react with sulfur or H_2S at elevated temperatures.

Most of the present nanocapsules have MoS_2 shells with thickness ranging from 6 to 11 nanometers. Therefore, if the size of the precursor metal nanoparticles were small enough, a complete transformation of the metal core to its sulfide would be expected. These stuffed fullerene-like nanoparticles, which are different from the most intensively studied hollow MoS_2 nanoparticles [4, 5], might involve different properties

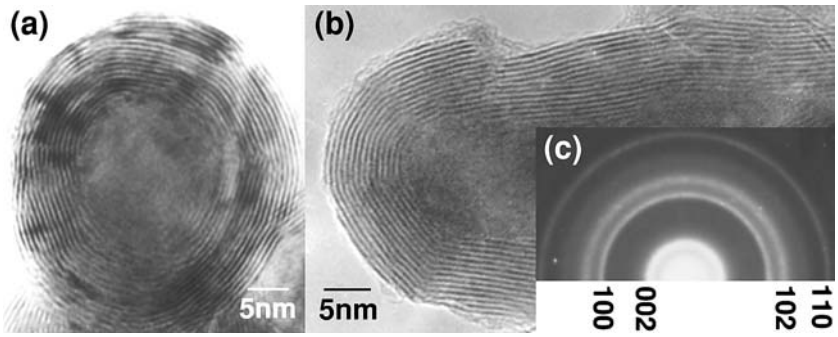

Figure 3 TEM images of multi-layered MoS_2-coated Mo/MoO_2 nanocapsules: (a) Isolated spherical nanocapsules; (b) elongated tubular nanocapsules; (c) shows electron diffraction pattern of the sample, which correspond to the (002), (100), (102) and (110) lattice planes of MoS_2.

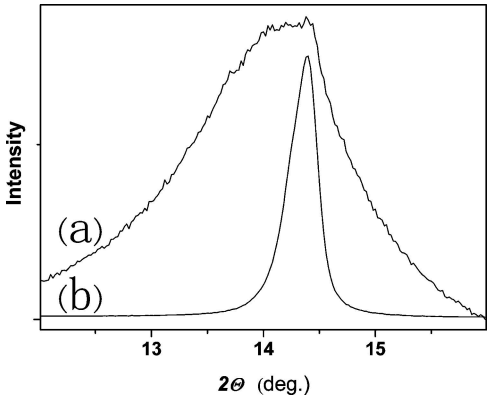

Figure 4 Normalized XRD patterns of the MoS_2 nanocapsules (a) and the commercial MoS_2 powders (b). The MoS_2 nanocapsules showed an average expansion of 1.2% along the *c* axis, compared with the bulk MoS_2. Peak splitting of (a) indicates varied inter-planar spacing of the MoS_2 shells.

and give us a way to study the stability of these folding structures.

The inter-planar spacing (Fig. 3) of the MoS_2 shell is 0.61 nm in general, which is consistent with that of the van der Waals gap of MoS_2 along the *c* axis. However, a detailed XRD investigation suggests an average expansion of 1.2% along the *c* axis compared with the bulk MoS_2, as indicated in Fig. 4. The expansion of the spacing of the two adjacent layers in the MoS_2 shell has been ascribed to the strain relief in the folded structure [12]. Compared with the 2% *c* axis expansion reported for the hollow MoS_2 nanoparticles prepared by the reaction between molybdenum oxide and H_2S with similar particle size [12], the 1.2% expansion of our sample is a little lower. We speculate the metallic core in our samples should be responsible for this difference. When the sulfur reacted with molybdenum beneath the previously formed MoS_2 layers, an additional strain force related to volume expansion from the interior is expected. The previously formed MoS_2 layers are obstacles to such volume expansion and therefore the expansion value is reduced.

Besides the general downward shift of the (0002) peak position of MoS_2 nanocapsules, a splitting of the peak has also been observed (Fig. 4), suggesting varied inter-layer spacing presented in the samples. This splitting is associated with the shape difference (for example, spherical and tubular) of different nanocapsules and therefore different strain relief of folded structures. Of course, the size distribution of these nanocapsules also results in an inter-planar spacing distribution.

The formation mechanism of the above MoS_2 nanocapsules encapsulating Mo/MoO should be quite different from that of the most extensively studied hollow MoS_2 nanoparticles produced by reducing molybdenum oxide, in which the sublimation of the molybdenum oxide is very important [5, 6, 12]. In this work, the high melting point of Mo and the low reaction-temperature used makes any volatility impossible. Thus the atom diffusion process must control the reaction between Mo and S. Taking advantage of the small size of the Mo particles, the reaction is quick enough for applications.

To clarify the role of H_2S during the synthesis, we have also conducted a similar experiment without the addition of H_2S. We find that the sulfur grows foams and overflows when heating, which makes further synthesis difficult. We believe that the hydrogen sulfide plays an important role in transferring excess sulfur out of the crucible and thus preventing the formation of sulfur foams. In fact, H_2S decomposes at 300°C according to $H_2S \leftrightarrow H_2 + S$, and the reaction is reversible. The temperature gradient in the reactor is important for the sulfur transportations. At high temperature region, H_2S decomposes and the resultant sulfur deposits on the cold wall of the reactor. As the reaction is going on, the excess sulfur will be continuously transferred to the low temperature region. The above reversible decomposition reaction of H_2S allows us to modulate the reaction time by modulating the amount of sulfur added and thus the thickness of the MoS_2 shells, because any excess sulfur can be transported out completely.

3.3. Single-layered WS_2(W) nanoparticles

TEM observations show that most of the W nanoparticles generated by using arc discharge method in H_2S are spherical in shape, with an average diameter of 15 nm. It is interesting to note that a single layer of WS_2 sheet covers most of the spherical nanoparticles, as shown in Fig. 5. The formation of the single-layered WS_2 shell, instead of multi-layered one, should be attributed to the fast movements of the nanoparticles from the high temperature arc region to the water-cooled chamber wall. We speculate the single-layered WS_2 shells are formed at the high temperature region of the arc. The high temperature of the arc can not only evaporate the W, but

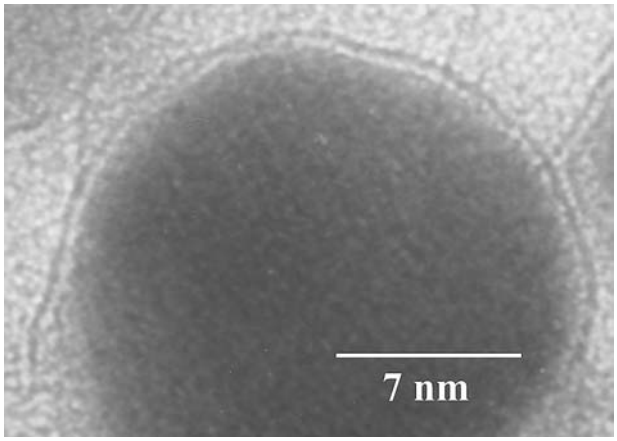

Figure 5 TEM images of single layered WS_2 encapsulating W nanocapsules.

also decompose the H_2S into sulfur and hydrogen. The evaporated W would react with the decomposed S in the arc region. Once the W nanoparticles left the arc region, the reaction would stop because of the low temperature.

4. Conclusions

CoS/CoO and Mo/MoO_2 nanoparticles have been successfully filled in the WS_2 and MoS_2 fullerene-like nanocages, respectively. The usage of metal nanoparticles as precursors and the doping method presented here not only result in a high yield of WS_2 and MoS_2 nanocapsules stuffed with different materials, but also in the minimized consumption of H_2S, which is a highly toxic gas to human health and polluting material to environment. Although our study focuses on WS_2 and MoS_2, analogous reactions can be extended to the large-scale synthesis of other metal dichalcogenide nanomaterials. Single layered WS_2 naocapsules encapsulating W have been prepared successfully by using the arc discharge method.

Acknowledgement

We gratefully acknowledge the suggestions from Dr. E. Brück in Van Der Waals Zeeman Institute, University of Amsterdam, and the financial supports from the National Natural Science Foundation of China (Grants Nos.59 725 103 and 50 171 070) and Technology Commission of Shenyang.

References

1. Z. D. ZHANG, in "Encyclopedia of Nanoscience and Nanotechnology" (American Scientific Publishers, California, 2003) *Nanocapsules*.
2. P. Z. SI, Z. D. ZHANG, D. Y. GENG, C. Y. YOU, X. G. ZHAO and W. S. ZHANG, *Carbon* **41** (2003) 247.
3. P. Z. SI, M. ZHANG, C. Y. YOU, D. Y. GENG, J. H. DU, X. G. ZHAO, X. L. MA and Z. D. ZHANG, *J. Mater. Sci.* **38** (2003) 689.
4. L. RAPOPORT, Y. BILIK, Y. FELDMAN, M. HOMYONFER, S. R. COHEN and R. TENNE, *Nature* **387** (1997) 791.
5. Y. FELDMAN, G. L. FREY, M. HOMYONFER, V. LYAKHOVITSKAYA, L. MARGULIS, H. COHEN, G. HODES, J. L. HUTCHISON and R. TENNE, *J. Am. Chem. Soc*. **118** (1996) 5362.
6. Y. FELDMAN, A. ZAK, R. POPOVITZ-BIRO and R. TENNE, *Solid State Sci*. **2** (2000) 663.
7. M. J. YACAMAN, H. LOPEZ, P. SANTIAGO, D. H. GALVAN, I. L. GARZON and A. REYES, *Appl. Phys. Lett*. **69** (1996) 1065.
8. Y. MASTAI, M. HOMYONFER, A. GEDANKEN and G. HODES, *Adv. Mater*. **11** (1999) 1010.
9. A. A. YARON, C. L. CLEMENT and J. L. HUTCHISON, *Electrochem. Solid-State Lett*. **2** (1999) 627.
10. M. REMSKAR, A. MRZEL, Z. SKRABA, A. JESIH, M. CEH, J. DEMSAR, P. STADELMANN, F. LEVY and D. MIHAILOVIC, *Science* **292** (2001) 479.
11. R. N. VISWANATH and S. RAMASAMY, *J. Mater. Sci*. **25** (1990) 5029.
12. Y. FELDMAN, E. WASSERMAN, D. J. SROLOVITZ and R. TENNE, *Science* **267** (1995) 222.

Received 30 September 2003
and accepted 18 March 2005